

AN EVALUATION OF LEAST-SQUARES AND CLOSED-FORM
DUAL-ANGLE METHODS FOR CODAR
SURFACE-CURRENT APPLICATIONS

DONALD E. BARRICK and BELINDA J. LIPA

Reprinted from IEEE Journal of Oceanic Engineering, Vol. OE-11, No. 2, April 1986

An Evaluation of Least-Squares and Closed-Form Dual-Angle Methods for CODAR Surface-Current Applications

DONALD E. BARRICK, MEMBER, IEEE, AND BELINDA J. LIPA

(Invited Communication)

Abstract—Extraction of surface currents from first-order CODAR sea echo requires use of a model that allows signals from two bearings to contribute to the Doppler spectrum at a given frequency. This is called the dual-angle situation, and it applies over much of the coverage area. Two dual-angle techniques have appeared in the literature: a least-squares algorithm used with a crossed-loop antenna system, and a closed-form approach applied to a four-element square array. We evaluate these methods against realistic signal and noise scenarios encountered in CODAR operations, and study nonstatistical biases remaining after infinite-ensemble averaging of the input voltage cross-spectral data. Based on these simulations, biases produced with the closed-form methods exceed those for the crossed-loop system analyzed with least squares by typically 150 percent.

I. INTRODUCTION

CODAR includes HF radars with compact receiving antenna systems that measure ocean surface parameters such as surface current velocities, wave-height directional spectra, and drifting transponder or ice-floe positions and speeds. These compact antennas form broad beams with limited angular resolution. Hence, specific surface information having high angular accuracy is extracted from the antenna signals by fitting models that are solutions for the scattered echo to the measured data. The process is analogous to pitch-roll buoys, for example, which have angular resolutions no better than 120° , but whose processed signals can provide swell directions to $1\text{--}2^\circ$ accuracy in bearing. The roles of the CODAR antenna and the ensuing data analysis are central to extraction of surface current maps, the original application of the system. Although a decade has passed since the first CODAR current maps were published [1], the issues regarding bearing accuracy and its impact on current products still remain unresolved. Significant positional biases in current maps produced by the older four-element system operated by the National Oceanic and Atmospheric Administration/Wave Propagation Laboratory (NOAA/WPL) have recently been reported [2], indicating problems of this nature.

The solution for the first-order Bragg-backscattered echo spectrum for CODAR [3] relates the signal at a given Doppler frequency to the current's radial velocity pattern. For typical

circulation patterns, it is shown that one or two signals with the same radial velocity can contribute to the Doppler spectrum at each frequency. Hence, the analysis for current extraction is reduced to finding one or two directions of arrival from the measured complex antenna element voltage frequency transforms at a given Doppler shift or radial velocity. These are referred to as "single" and "dual" angle models. For coastal operation of CODAR, the single-angle model can be used with confidence everywhere *only when flow is parallel to a straight coastline*, as can be seen by examining the radial velocity pattern versus bearing angle for this case. Any more general arbitrary current patterns will require a dual-angle model over at least part of the CODAR coverage area. When the system is operated from an offshore platform with water completely surrounding it, simple geometric considerations show that the dual-angle model must be used nearly 100 percent of the time. We have found that even for coastal operations, the dual-angle model is applicable and required over *at least* 40 percent of the coverage area. Therefore the use of an accurate dual-angle model is critical to successful CODAR operations for surface current mapping everywhere.

We published and demonstrated least-squares methods for both single- and dual-angle analysis of CODAR signals in [3]. The only other published dual-angle technique valid for signals that can arrive over 360° has recently appeared [4]. (A dual-angle solution for CODAR was derived within NOAA in [5] and repeated in [6]; the derivation is incorrect, however, and the results have not been published.) The method presented in [4] applies to a four-element square receiving antenna array and is called "closed form" because expressions for the two angles of arrival are obtained directly from the complex voltages at the four antennas. The method is exact in the absence of noise and errors, and when precisely only two signals are present; the method is known to have instabilities, i.e., regions of bearings where the closed-form solutions fail. Furthermore, since the problem is overdetermined, i.e., there are considerably more data samples available than there are parameters sought from the analysis, the method of [4] produces four different sets of closed-form solutions for the same two angles. When noise is present, all four of these solution sets will be different.

In [3], we showed that the optimum method for processing noisy CODAR data—from either crossed-loop antenna sys-

Manuscript received August 23, 1985; revised January 16, 1986.
D. E. Barrick is with Ocean Surface Research, Boulder, CO 80303.
B. J. Lipa is with Ocean Surface Research, Woodside, CA 94062.
IEEE Log Number 8608312.

tems or from the four-element square antenna arrays both used for CODAR—is maximum likelihood; this reduces to least squares for sea-echo data signals. This method also allows objective determination of whether the single- or dual-angle model best fits the data and gives the statistical uncertainties associated with all output products, which the closed-form methods do not provide. On the other hand, it is not a closed-form solution, and requires a search for a minimum by some means over both bearing angles. Closed-form solutions have a certain appeal, and the question arises, how much less than “optimum” are they? 2 percent? 10 percent? 25 percent? Since both sets of analysis methods have now appeared [3], [4], our purpose here is to compare them by applying them both to the same input data. Our intentions are a) to provide the potential user with information that will allow selection of which techniques are better suited to a given application; and b) to give sufficient detail here so that our simulations can be verified and extended, if desired. Because the four-element antenna array is known to produce sidelobe biases and mutual coupling [3], [7], we will compare the least-squares methods of [3] applied to the crossed-loop system with the closed-form methods of [4] applied to the four-element array; both antenna systems have been used extensively in the past, and hence, such comparisons should prove meaningful to interested users. The types of bearing errors examined here are biases that remain after an infinite ensemble average of input data samples; hence, statistical fluctuations are no longer present in the biases. Although it would be desirable to have both CODAR’s, each with its different antenna system and processing method, sitting side by side in an experiment measuring the same actual sea-echo signals, such a plan would be quite expensive and inconclusive, because the current field each is attempting to measure is not precisely known. Consequently, we resort to simulations, using known input along with our best estimates (based on experience) of typical dual-angle coastal signal-noise scenarios.

II. SIMULATIONS

A. The Signal-Noise Model

After Fourier transforming measured received time-series voltages from the antenna elements, the two peak regions comprising the first-order sea echo are identified [3]. The voltages at a given frequency in this region, to be used for current extraction, are taken to consist of two signals from different directions, along with additive noise. Since we are considering coastal applications here, we restrict the signal directions to 180° of space, i.e., $-90^\circ < \theta_1, \theta_2 < 90^\circ$. Both signal and noise voltages are Gaussian random variables [3]. At HF, the noise is known to be external, and our studies [3] have shown typical average noise levels to lie between 5 and 15 dB below the desired sea-echo signal levels, *at all ranges* from the radar. This suggests that the “noise” seen is actually produced by the transmitted signal, i.e., some type of “clutter” originating from moving ocean waves (possibly higher order scatter), since the noise level with the transmitter turned off is 50–60 dB lower than the signal levels for most radar ranges. If so, this noise must be somewhat directional,

also originating out over the sea.

Both techniques that have been proposed [3], [4] recommend the use of preaveraged cross spectra among the antenna voltages; when the voltages themselves are Gaussian, such cross spectra are generalized chi-squared random variables with $2N$ degrees of freedom, where N is the number of samples used in the preaverage [3]. Error in extracted angles will then consist of two components as a result of the noise: 1) the statistical fluctuation about a mean due to the fact that only N samples were averaged rather than an infinite number; and 2) a residual mean bias based on how the antenna and extraction algorithm respond to signal plus noise. The former fluctuation is well understood, and for both techniques and systems the output statistical fluctuation decreases as $1/\sqrt{N}$ for N larger than ~ 5 [3], [8]; hence, we deal with only the second type of bias error in this paper. Therefore the complex *infinite-ensemble* averaged voltage cross spectra for both systems $\langle V_i V_j^* \rangle$ will consist of three terms 1) the signal of power P_1 originating from bearing θ_1 ; 2) the signal of power P_2 originating from direction θ_2 ; 3) the noise term having power N_0 . In this we assume that the sea-echo signals originating from different directions are uncorrelated with each other and with the noise signals; hence, phase differences among them disappear in the infinite-ensemble averaging process. For our simulations here, we employ as input $P_1 = P_2 = 1$. Hence, $1/N_0$ is the average signal-to-noise ratio, and we take this to be 10 (10 dB) as midway in the typical range of values we encounter in HF operations.

We use two noise models; both assume uniformly distributed noise over some bearing sector of width 2γ centered on θ_0 , whose infinite-ensemble contribution to the i - j th cross spectrum is

$$\langle V_i V_j^* \rangle|_{\text{Noise}} = (N_0/2\gamma) \int_{\theta_0-\gamma}^{\theta_0+\gamma} a_i(\theta) a_j^*(\theta) d\theta \quad (1)$$

where $a_i(\theta)$ is the normalized complex pattern of the i th antenna element with respect to the antenna system center. Thus, for example, in the NOAA/WPL four-element square monopole array of [4], $a_1(\theta)$ is the phasor response of Element #1 given by [4, eq. (5)] as $a_1(\theta) = \xi = \exp(ikr \sin \theta)$, where k is the radar wavenumber ($2\pi/\lambda$ with λ being the radar wavelength); Element #1 is located a distance r from the origin at the array center along the $+x$ axis, with #2, 3, and 4 at equal distances on the $+y$, $-x$, and $-y$ axes, respectively. For the crossed-loop system, $a_i(\theta)$ are $\cos \theta$, $\sin \theta$, or 1 for the two loops and monopole elements, respectively [3], where the Loop #1 positive lobe points along the $+x$ axis and the Loop #2 lobe along the $+y$ axis. Assumed in the use of (1) above is the fact that noise voltages from different directions within the sector are mutually uncorrelated, keeping with the definition of [3, eq. (6)] and the assumption made also in [4, sec. IV]. The first noise model we employ assumes $\gamma = \pi$, i.e., noise isotropically distributed over 360° . This case is illustrated in Fig. 1; it is identically the noise model used in [4] in the limit of infinite samples for the noise distribution. The second model takes the noise as originating from the quadrant over the sea defined by $\gamma = \pi/4$ (Fig. 2). This moderately directional

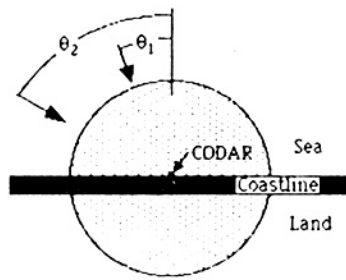


Fig. 1. Geometry for coastal CODAR operation with two sea-echo signals and isotropic noise from 360° (shown as shaded circle).

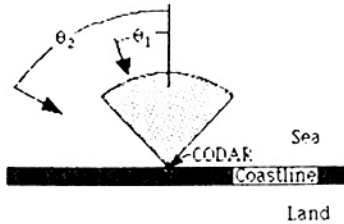


Fig. 2. Geometry for coastal CODAR operation with two sea-echo signals and uniform noise from north quadrant over the sea (shown shaded).

model is probably more realistic than the isotropic model for coastal CODAR operation for the reasons discussed earlier. Nonetheless, *neither* can be assumed to represent the noise situation in general, and each is used here only to allow comparisons with reasonably typical conditions.

B. The Antenna Systems and Extraction Algorithms

1. The Four-Element Monopole Array and Closed-Form Solutions [4]: This system is described in [4] as it would operate under perfect conditions. Four monopole elements are arranged in a square of radius r , with patterns that are taken to be omnidirectional. Hence, mutual coupling and other forms of pattern distortion that are known to bias recovered bearings [7] are neglected in [4] and here also. Assuming two signals from θ_1 and θ_2 with no noise present, expressions are derived in [4, eq. (31)] that—used in the quadratics as given in (11) and (12) there—lead to eight possible solutions for the recovered angles θ_i . The results can be written functionally for the eight angles as $(\theta_{1n}, \theta_{2n}) = f_n(\tau)$, for $1 \leq n \leq 4$, with $f_n(\tau)$ being one of four closed-form nonlinear solutions for the angles given in [4]; τ is the 4×4 measured averaged input data matrix whose typical element $\tau_{ij} = \langle V_i V_j^* \rangle$ is the cross spectrum of the i, j th antenna voltages ($1 \leq i, j \leq 4$). With no noise present, these four angle pairs are the same, i.e., identically the four input pairs θ_1, θ_2 . With noise present, the four solution pairs will in general all be different; the measure of bias is the difference between them and the input angles. The noise term for the first (isotropic) model that must be added to the cross spectra in the simulation is N_0 for the self spectra τ_{ii} ; $N_0 J_0(\sqrt{2}kr)$ for $\tau_{12}, \tau_{43}, \tau_{14},$ and τ_{23} ; $N_0 J_0(2kr)$ for τ_{13} and τ_{24} ; where $J_0(x)$ is the Bessel function of the first kind of order zero and argument x . In the case of the isotropic noise model, we consider two array radii: $r = \lambda/4$ and $r = \lambda/8$. The NOAA/WPL CODAR has historically used a spacing between these two values (but closer to $\lambda/4$) for all operations.

For the quadrant noise model, we employ the array radius $r = \lambda/4$. The same noise constant N_0 is added to the self-spectra; the quantity $(.0978 \pm i.7693)N_0$ is added to τ_{12}, τ_{43} and τ_{14}, τ_{23} , respectively; $(.2980 + i0.0)N_0$ is added to τ_{13} ; and $(-.9033 - i.3044)N_0$ is added to τ_{24} . These constants are obtained by performing the integrations indicated in (1) numerically. As N_0 went to zero, the results of the algorithm were checked to verify that the dual-angle closed-form solutions indeed gave the correct answers.

2. The Crossed-Loop System and Least-Squares Algorithm [3]: The least-squares dual-angle solution in its basic form, given in ([3], eq. (32)) is expressed functionally as $[b - m]^T [b - m] \Rightarrow \text{minimum}$, where b is the 5×1 trigonometric Fourier angular coefficient matrix of the input data (with m the 5×1 model matrix) whose elements are given in terms of the averaged cross spectra among the three antenna elements ($b_n \sim \langle V_i V_j^* \rangle$, for $-2 \leq n \leq +2$ and $1 \leq i, j \leq 3$) in [3, eq. (16)] with one exception; the trigonometric Fourier angular coefficients b_n are normalized by dividing by the constants q_n , and, hence, q_n no longer appears in [3, eq. (32)]. (This has been done in the real-time current-extraction software implementation of the methods of [3] and reflects the statement before section C [3, p. 233] that the terms of the least-squares sum are to be weighted equally in terms of the voltage cross spectra that comprise them.) The noise model counterpart of (1) here is then written as

$$b_n |_{\text{Noise}} = (N_0/2\gamma) \int_{\theta_0-\gamma}^{\theta_0+\gamma} t f_n(\theta) d\theta \quad (2)$$

where $t f_n(\theta)$ are the $\cos(n\theta)$ and $\sin(n\theta)$ basis functions used in that analysis. Then, to represent the noise input for the simulations, we add only N_0 to b_0 for the isotropic model; for the quadrant noise model we add N_0 to b_0 , $N_0\sqrt{8}/\pi$ to b_1 , and $2N_0/\pi$ to b_2 . The two signals (with unity power amplitudes) used as input for b_n are then $t f_n(\theta_1) + t f_n(\theta_2)$.

Unlike the closed-form algorithms derived and used from [3], the least-squares solution can incorporate a model for noise in the minimization process, as discussed and demonstrated in [3]. In these simulations, if we include exactly the same noise model as the input, we will of course obtain the original input angles with no errors or biases; this would not be a fair simulation, for a) the details of the noise model to be encountered at a given time are not known ahead of time; and b) the number of parameters that can be used to describe an arbitrary noise model are limited, in that the *total* number of parameters sought in the minimization cannot exceed the number of data samples. Hence, for the case of isotropic input noise, we use *no* noise model in the least-squares minimization; this is therefore similar to ignoring the noise, as done in the closed-form solutions with which it is compared. For the case of quadrant noise input, we use least squares in two ways: 1) with no noise model in the extraction process; and 2) with a one-parameter model that represents uniformly distributed noise coming from the half-space over the sea.

Thus four (or in the latter case, five) parameters are sought in the least-squares minimization process: two positive signal powers and two angles (and N_0 in the latter case). The

minimum is found by eliminating the two (or three) linear power factors and doing a simple grid search for the remaining two angles. In keeping with the operation of the real-time software implementation of this process [3], the grid search is done in 5° angular increments. It is recognized that many search algorithms are available to find a minimum exactly in multidimensional space (e.g., the "Simplex" search [9]); it being very robust and reliable, we have found the simple grid search to be of sufficient speed and accuracy for normal CODAR operations, so that use of these more precise methods has not been warranted.

C. Results

We present the results of the simulations in Tables I-IV. We thought it more illuminating to present the actual solutions obtained by the various methods, rather than combining them as histograms or scatter plots. In this manner, angular regions of greater biases can be identified. In all cases, the recovered solutions were paired in the most favorable manner in these tables with respect to the input pair. In the case of isotropic noise, there is considerable symmetry; hence, although only 22.5° was used as the θ_1 input angle, this can represent 67.5°, -22.5°, -67.5°, etc., by reflections about the 45° bearings. On the other hand, for noise coming from the north quadrant, the biases in the recovered data differ considerably for θ_1 of 22.5° and 67.5°; hence both are examined. The one input angle is taken as 22.5° or 67.5°, rather than falling precisely on the 15° steps of the second angle for two reasons: 1) the dual-angle closed-form solutions are known to be unstable (i.e., singular) when the two angles are exactly equal, and hence we wanted to avoid this condition so as not to bias the output of that method pessimistically; and 2) with the first angle selected in this manner, the grid search at 5° increments is not overly favored because one of the angles will always fall precisely between two grid points as noise goes to zero.

Finally, we give the standard deviations of the recovered pair angles of each column from the input angles as σ . In the case of the least-squares solutions obtained by the grid-search method quantized every 5°, we also give as σ_0 the standard deviation when the quantizing "noise" is removed, as for example, if an exact minimum-finder were used.

III. DISCUSSION AND CONCLUSIONS

a) In all except one case, the simulations show much greater biases for the dual-angle solutions with the four-element system. Bearing errors based on the latter are usually worse by a factor of 2.5.

b) The four closed-form solutions generally differ from each other, with some being in greater error than others. There is no objective way to select the better of these solutions because they depend on the noise input, and noise parameters cannot be determined from these closed-form solutions.

c) Both techniques and systems display the greatest biases when the two angles tend to approach each other, i.e., merging to the single-angle situation. The angular width of this sector of bad biases is much greater for the closed-form solutions, exceeding half the coastal angular coverage over the ocean in certain situations.

TABLE I
COMPARISONS OF INPUT AND RECOVERED ANGLES (IN DEGREES) USING LIPA-BARRICK LEAST-SQUARES SOLUTION FOR CROSSED-LOOP ANTENNA SYSTEM (NO-NOISE MODEL) AND MILLER-LYONS-WEBER CLOSED-FORM SOLUTIONS FOR FOUR-ELEMENT SQUARE ANTENNA SYSTEM WITH $\lambda/4$ ARRAY RADIUS. BOTH SIGNALS OF DUAL-ANGLE FORMULATION HAVE EQUAL AMPLITUDES; ISOTROPIC NOISE FROM 360° ASSUMED, WITH 10-dB SIGNAL-TO-NOISE RATIO.

Input Angles	Lst-Sqrs Solution	Miller - Lyons - Weber Closed-Form Solutions			
		Solution #1	Solution #2	Solution #3	Solution #4
22.5 -90.0	20 -90	22.9 -89.3	22.8 -89.0	22.9 -89.3	22.8 -89.0
22.5 -75.0	25 -75	22.9 -74.4	22.8 -74.2	22.9 -74.4	22.8 -74.2
22.5 -60.0	25 -60	23.0 -59.6	23.0 -59.4	23.0 -59.6	22.9 -59.4
22.5 -45.0	25 -45	23.0 -45.0	23.0 -44.7	23.2 -45.0	22.9 -44.7
22.5 -30.0	25 -30	22.6 -31.1	23.0 -30.1	23.5 -31.3	22.1 -29.9
22.5 -15.0	25 -15	21.8 -15.4	22.7 -15.8	21.8 -13.8	25.6 -17.3
22.5 0.0	20 -10	21.7 -5.9	21.3 -2.7	20.2 -0.6	25.6 -8.0
22.5 15.0	40 15	22.9 20.3	20.2 0.0	18.8 1.8	21.6 19.4
22.5 30.0	5 30	27.2 36.1	2.6 27.1	6.8 26.6	27.7 34.7
22.5 45.0	25 55	-3.2 39.8	13.9 38.6	14.4 38.5	-3.8 39.9
22.5 60.0	20 60	1.0 52.0	13.1 50.2	13.3 50.2	3.9 52.0
22.5 75.0	20 75	29.8 80.5	28.0 83.3	28.0 83.4	29.8 80.4
22.5 90.0	20 90	21.4 91.3	23.8 91.7	23.8 91.7	21.4 91.2
	$\sigma = 5.8^\circ$	$\sigma = 7.1^\circ$	$\sigma = 6.4^\circ$	$\sigma = 5.5^\circ$	$\sigma = 7.3^\circ$
	$\sigma_0 = 5.5^\circ$				

TABLE II
SAME AS TABLE I, BUT WITH $\lambda/8$ FOUR-ELEMENT ARRAY RADIUS

Input Angles	Lst-Sqrs Solution	Miller - Lyons - Weber Closed-Form Solutions			
		Solution #1	Solution #2	Solution #3	Solution #4
22.5 -90.0	20 -90	22.7 -90.8	22.5 -90.2	22.8 -90.7	22.4 -90.3
22.5 -75.0	25 -75	22.8 -75.5	22.7 -74.8	23.0 -75.4	22.5 -75.9
22.5 -60.0	25 -60	22.8 -60.5	22.8 -59.3	23.2 -60.4	22.3 -59.4
22.5 -45.0	25 -45	22.3 -46.6	22.6 -44.0	23.7 -46.5	21.2 -43.9
22.5 -30.0	25 -30	23.7 -53.5	22.1 -28.8	29.7 -52.0	14.0 -25.5
22.5 -15.0	25 -15	6.6 6.6	20.3 -14.2	13.3 -6.7	14.4 -1.4
22.5 0.0	20 -10	22.8 12.0	17.5 1.9	14.5 -6.3	28.0 15.1
22.5 15.0	40 15	72.7 18.7	39.4 19.6	33.8 -34.5	47.6 31.4
22.5 30.0	5 30	26.2 58.1	26.9 41.8	-15.3 38.6	35.3 47.5
22.5 45.0	25 55	34.8 52.7	20.4 35.3	10.4 35.0	35.1 52.0
22.5 60.0	20 60	45.3 90.2	9.7 44.1	10.2 44.1	45.3 90.7
22.5 75.0	20 75	37.9 84.0	33.6 111.1	33.8 111.5	37.8 83.6
22.5 90.0	20 90	26.4 91.4	23.7 93.4	23.9 93.8	26.2 91.0
	$\sigma = 5.8^\circ$	$\sigma = 16.1^\circ$	$\sigma = 9.7^\circ$	$\sigma = 16.3^\circ$	$\sigma = 12.4^\circ$
	$\sigma_0 = 5.5^\circ$				

d) Decreasing the array spacing of the four-element antenna aggravates the errors for the dual-angle situation, in contrast with its effect with the single-angle solution modeled in [7] where decreased size appeared to eliminate sidelobe biases.

e) The least-squares process allows for a noise model to be fitted to the data along with the two signals. The use of any model that better describes the physical processes involved will reduce the errors in extracted bearings. Although only a preliminary look at including some form of noise model has been undertaken thus far, this would appear to be a fruitful area for further study. At least the least-squares method admits this possibility, whereas the closed-form algorithms preclude it.

f) In the analysis performed here, it is not generally possible to separate the effect of the analysis method from the antenna system with which it was used; this was found to be true also in [3] and [7]. Hence, we cannot quantitatively say at this point how much better the four-element array system would have performed had least-squares methods been used. However, it is clear that even in the latter case, sidelobes remain a problem [3] and will certainly be a source of bias not found with the crossed-loop system.

g) Reiterating our claim in the Introduction, no current-extraction software for CODAR can reproduce the typical

TABLE III
COMPARISONS OF INPUT AND RECOVERED ANGLES (IN DEGREES) USING LIPA-BARRICK LEAST-SQUARES SOLUTION FOR CROSSED-LOOP ANTENNA SYSTEM AND MILLER-LYONS-WEBER CLOSED-FORM SOLUTIONS FOR FOUR-ELEMENT SQUARE ANTENNA SYSTEM WITH $\lambda/4$ ARRAY RADIUS. LEAST-SQUARES FORMULATION EMPLOYS BOTH NO-NOISE MODEL AND A HALF-SPACE NOISE MODEL. BOTH SIGNALS OF DUAL-ANGLE FORMULATION HAVE EQUAL AMPLITUDES. UNIFORM NOISE COMES FROM NORTH QUADRANT OVER THE SEA, WITH 10-dB SIGNAL-TO-NOISE RATIO. FIRST SIGNAL IS FROM 22.5°.

Input Angles	Least-Squares Solutions			Miller - Lyons - Weber Closed-Form Solutions			
	No Noise	Hf-Spc Noise		Solution #1	Solution #2	Solution #3	Solution #4
22.5 -90.0	20 -90	20 -90		22.0 -88.4	22.0 -88.4	22.0 -88.4	22.0 -88.4
22.5 -75.0	20 -75	20 -75		22.0 -73.9	21.9 -73.9	22.0 -73.9	21.9 -73.9
22.5 -60.0	20 -60	20 -60		22.1 -59.1	22.1 -59.1	22.1 -59.1	22.1 -59.1
22.5 -45.0	20 -45	20 -45		22.3 -44.4	22.3 -44.4	22.3 -44.4	22.3 -44.4
22.5 -30.0	30 -25	20 -30		22.5 -29.8	22.5 -29.8	22.5 -29.8	22.5 -29.8
22.5 -15.0	30 -10	20 -15		22.5 -15.5	22.5 -15.5	22.5 -15.5	22.5 -15.5
22.5 0.0	25 0	20 -5		21.2 -3.1	21.1 -3.1	21.1 -3.0	21.2 -3.2
22.5 15.0	25 10	20 0		19.6 -12.7	19.5 -11.5	19.4 -8.3	19.7 -15.7
22.5 30.0	10 30	20 30	-13.8 26.7	-12.9 26.6	-10.9 26.6	-15.7 26.7	
22.5 45.0	10 40	10 40	6.6 38.6	7.9 38.4	8.0 38.4	6.5 38.6	
22.5 60.0	20 60	20 60	8.5 51.3	9.6 51.1	9.6 51.1	8.5 51.3	
22.5 75.0	20 75	20 75	33.6 88.9	33.3 89.8	33.3 89.8	33.6 88.9	
22.5 90.0	20 90	20 90	23.9 92.3	23.7 92.4	23.7 92.4	23.8 92.3	
	$\sigma = 4.8^\circ$	$\sigma = 4.4^\circ$	$\sigma = 10.7^\circ$	$\sigma = 10.5^\circ$	$\sigma = 10.0^\circ$	$\sigma = 11.3^\circ$	
	$\sigma_o = 4.4^\circ$	$\sigma_o = 4.0^\circ$					

TABLE IV
SAME AS TABLE III, BUT FIRST SIGNAL IS FROM 67.5°

Input Angles	Least-Squares Solutions			Miller - Lyons - Weber Closed-Form Solutions			
	No Noise	Hf-Spc Noise		Solution #1	Solution #2	Solution #3	Solution #4
67.5 -90.0	65 -85	65 -90		65.6 -89.9	65.2 -89.3	64.6 -90.7	66.3 -88.5
67.5 -75.0	65 -75	65 -75		65.1 -75.1	65.7 -73.6	65.2 -75.0	65.6 -73.6
67.5 -60.0	65 -60	70 -60		66.9 -58.0	66.1 -58.4	66.2 -58.1	66.8 -58.2
67.5 -45.0	65 -45	70 -45		66.4 -43.5	66.3 -43.6	66.3 -43.5	66.4 -43.6
67.5 -30.0	65 -30	65 -30		66.5 -29.1	66.4 -29.1	66.4 -29.1	66.5 -29.1
67.5 -15.0	65 -15	70 -10		66.6 -15.0	66.5 -15.0	66.5 -15.0	66.6 -15.0
67.5 0.0	70 0	65 -5		66.1 -1.3	66.1 -1.3	66.1 -1.3	66.1 -1.3
67.5 15.0	65 10	65 10		61.6 7.9	61.4 8.2	61.4 8.2	61.6 7.9
67.5 30.0	60 15	65 25	98.4 45.5	100.9 45.3	100.9 45.3	98.4 45.5	
67.5 45.0	60 15	65 15	101.7 51.1	105.1 51.0	105.1 51.0	101.7 51.1	
67.5 60.0	70 45	65 30	63.2 -15.5	63.2 -13.2	63.2 -13.1	63.2 -15.5	
67.5 75.0	40 75	55 75	-16.9 70.4	-14.7 70.4	-14.7 70.4	-16.8 70.4	
67.5 90.0	45 85	50 85	70.7 99.6	70.5 100.3	70.4 100.5	70.8 99.5	
	$\sigma = 10.5^\circ$	$\sigma = 9.7^\circ$	$\sigma = 24.4^\circ$	$\sigma = 24.1^\circ$	$\sigma = 24.2^\circ$	$\sigma = 24.4^\circ$	
	$\sigma_o = 10.3^\circ$	$\sigma_o = 9.3^\circ$					

circulation patterns encountered in coastal operations unless it includes an accurate dual-angle algorithm, since our experience shows that over 40 percent of the angular coverage area is dominated by dual-angle cases. For offshore platform operations with CODAR, this figure approaches 100 percent. Hence, the need for an accurate objective dual-angle antenna/algorithm for CODAR current mapping is essential, and provided the impetus for the present analysis.

ACKNOWLEDGMENT

The authors wish to express our sincere appreciation to our colleagues P. A. Miller, R. S. Lyons, and B. L. Weber of NOAA/WPL for discussions on the features and merits of the various angle extraction methods that supported our investigation here.

REFERENCES

- [1] D. E. Barrick, M. W. Evans, and B. L. Weber, "Ocean surface currents mapped by radar," *Science*, vol. 198, pp. 138-144, 1977.
- [2] F. Schott, A. S. Frisch, K. Leaman, G. Samuels, and I. Popa Fotino, "High-frequency Doppler radar measurements of the Florida Current in summer 1983," *J. Geophys. Res.*, vol. 90, no. C5, pp. 9006-9016, 1985.
- [3] B. J. Lipa and D. E. Barrick, "Least-squares methods for the extraction of surface currents from CODAR crossed-loop data: Application at ARSLOE," *IEEE J. Ocean. Eng.*, vol. OE-8, no. 4, pp. 226-253, Oct. 1983.
- [4] P. A. Miller, R. S. Lyons, and B. L. Weber, "A compact direction-finding antenna for HF remote sensing," *IEEE Trans. Geosci. Remote Sensing*, vol. GE-23, no. 1, pp. 18-24, Jan. 1985.
- [5] B. L. Weber and L. A. Leise, "A four-element direction-finding antenna," NOAA, Boulder, CO, Tech. Memo. ERL WPL-99, 1982.
- [6] T. M. Georges, Ed., *Coastal Ocean Dynamics Applications Radar: A User's Guide*, NOAA Wave Propagation Lab., Boulder, CO, Nov. 1984.
- [7] D. E. Barrick, "CODAR directional biases with a 4-element antenna array," *IEEE Trans. Geosci. Remote Sensing*, vol. GE-24, no. 3, pp. 415-420, May 1986.
- [8] D. E. Barrick, "Accuracy of parameter extraction from sample-averaged sea-echo Doppler spectra," *IEEE Trans. Antennas Propagat.*, vol. AP-28, no. 1, pp. 1-11, Jan. 1980.
- [9] J. C. Nash, *Compact Numerical Methods for Computers*. New York: Wiley, 1979.



Donald E. Barrick (M'62), for photograph and biography please see this issue, p. 146.



Belinda J. Lipa, for photograph and biography please see this issue, p. 245.